

Identification of favorable environments for thunderstorms in reanalysis data

ANJA T. WESTERMAYER^{1,3*}, PIETER GROENEMEIJER¹, GEORG PISTOTNIK^{1,4}, ROBERT SAUSEN² and EBERHARD FAUST³

¹European Severe Storms Laboratory e.V. (ESSL), Wessling, Germany

²Deutsches Zentrum für Luft und Raumfahrt (DLR), Institut für Physik der Atmosphäre, Oberpfaffenhofen, Germany

³Munich Re, München, Germany

⁴Zentralanstalt für Meteorologie und Geodynamik (ZAMG), Wien, Austria

(Manuscript received November 2, 2015; in revised form February 25, 2016; accepted February 29, 2016)

Abstract

The relations between lightning occurrence over Europe from the EUCLID network (2008–2013) and parameters derived from ERA-Interim reanalysis data were studied to increase the understanding of the conditions under which thunderstorms form. The objective was to identify relevant factors beyond instability and convective inhibition, in order to better model thunderstorms using numerical weather prediction or climate model data. It was found that latent instability is only required up to a certain amount of approximately 200–400 J kg⁻¹ CAPE. For higher values of CAPE (~ 800–2800 J kg⁻¹), the relative frequency of lightning is rather constant. Relative humidity in the low to mid-troposphere has a major influence on storm occurrence with low relative humidity strongly suppressing thunderstorm development. For an average 850–500 hPa relative humidity below 50 %, the frequency of lightning decreases to below 15 %, even when CIN is negligible and CAPE sufficient. A subtle dependency on wind shear was found in which two regimes of higher frequency of lightning were identified. For very weak and for high shear the probability was higher than for intermediate values of both deep-layer and low-level shear.

Keywords: convective initiation, thunderstorm, reanalysis

1 Introduction

An increasing number of studies address the impact of climate change on thunderstorms and their associated hazards, such as tornadoes, large hail, and wind gusts (e.g., TRAPP et al. 2007b; VAN KLOOSTER and ROEBBER 2009; DIFFENBAUGH et al. 2013; ALLEN et al. 2014; GENSINI and MOTE 2014; TIPPETT et al. 2015). The limited resolution (both temporally and spatially) of climate and reanalysis models does not allow an explicit simulation of thunderstorms, which poses a considerable challenge for such studies. TRAPP et al. (2007b) provided a proof-of-concept to dynamically downscale global climate simulations down to a horizontal grid spacing of 4 km or less at which convection does not need to be parameterized. Since then, a number of studies have used this technique (TRAPP et al., 2011; GENSINI and MOTE, 2014). However, high computational costs have prevented integrations at such resolutions over long time periods or across ensembles of climate models (GENSINI and MOTE, 2015). A less expensive method is the use of proxy parameters which are based on covariates that climate models are able to simulate (BROWN and MURPHY, 1996; BROOKS et al., 2003). Several researchers

have used proxies that are combinations of Convective Available Potential Energy (CAPE) and deep-layer wind shear (DLS; the bulk wind shear across the lowest 6 kilometers of the troposphere) (e.g., BROOKS et al. 2003; NIALL and WALSH 2005; TRAPP et al. 2007a; DEL GENIO et al. 2007; VAN KLOOSTER and ROEBBER 2009; SANDER 2011; SANDER et al. 2013; DIFFENBAUGH et al. 2013; ALLEN et al. 2014; TIPPETT et al. 2015) to model the occurrence of convective hazards in the present and/or future climate. In this study, we limit ourselves to modeling the occurrence of thunderstorms, regardless of the hazards that they produce. In other words, we are concerned with the question whether a lightning-producing storm will form in the first place, not considering whether it will produce phenomena like hail, tornadoes or severe winds gusts.

Among the covariates, CAPE represents the combination of the first two of the three *ingredients* that are required for deep, moist convection: i) instability (i.e. a strong decrease of temperature with height), ii) low-level moisture and iii) lift (MCNULTY, 1978; DOSWELL III, 1987; JOHNS and DOSWELL III, 1992; DOSWELL III et al., 1996; SCHULTZ et al., 2002).

All three ingredients are crucial for the initiation of deep moist convection and a lack of one of them might not result in any thunderstorm at all.

*Corresponding author: Anja T. Westermayer, European Severe Storms Laboratory e.V. (ESSL), Wessling, Germany, e-mail: anja.westermayer@physik.lmu.de

Authors concerned with storms that produce severe weather also considered DLS, because convective systems tend to become well-organized (e.g., WEISMAN and KLEMP 1984; THOMPSON et al. 2003) and therefore more likely to produce severe weather (e.g., CRAVEN and BROOKS 2004; GROENEMEIJER and VAN DELDEN 2007). Only little research has been done into the exact amount of instability required for a convective storm to become electrified and thus classify as a thunderstorm (e.g., BRIGHT et al. 2005; VAN DEN BROEKE et al. 2005). A guideline used at the United States Storm Prediction Center states that sufficient CAPE must be present to support vertical motions in excess of $6\text{--}7\text{ m s}^{-1}$ within the lower mixed-phase region of the cloud between $-10\text{ }^{\circ}\text{C}$ and $-20\text{ }^{\circ}\text{C}$ (BRIGHT et al., 2005). Theoretically this can be reached when $18\text{--}25\text{ J kg}^{-1}$ of CAPE are released in an updraft (VAN DEN BROEKE et al., 2005). BRIGHT et al. (2005) emphasized, that the actual updraft velocities are generally much less than the updraft velocities that are calculated by pure parcel theory and therefore suggests values for CAPE between 100 and 200 J kg^{-1} to be more realistic to ensure sufficient updraft strength.

It is important to mention that proxies that only include a measure of instability like CAPE (and possibly DLS) do not account for the third ingredient, lift. Therefore, they cannot predict whether convective initiation takes place and thereby release the CAPE in the first place.

To evaluate the formation of severe weather, WAPLER et al. (2015) used various observations that have a predictive skill for convective development, such as satellite-based cloud-top cooling rates, 3D-radar reflectivity, mesocyclone detection from doppler radar, lightning jumps or overshooting top detection.

VAN KLOOSTER and ROEBBER (2009) have modelled the probability of initiation using a neural network, TRAPP et al. (2007a) and TIPPETT et al. (2012) used the convective precipitation as a proxy. Others merely addressed the probability of initiation in a qualitative way. SANDER (2011) considered convective inhibition (CIN), but the authors did not quantify the probability of initiation explicitly as a function of CIN. Neither did DIFFENBAUGH et al. (2013), who, in a study of climate models from the Coupled Model Intercomparison Project Phase 5 (TAYLOR et al., 2012), studied changes in CIN on days on which the conditional probability of storms becoming severe was high. In fact, they acknowledged the limitation to their study that important meso- and synoptic scale processes that aid convection initiation are not explicitly captured by the parameters they addressed, including CIN.

Besides CIN and convective precipitation, other parameters may be considered as predictors for convective initiation, such as the humidity above the boundary layer. Observational evidence is provided by several authors, such as ZHANG and KLEIN (2010), who found that high humidity above the boundary layer precedes the onset of heavy precipitation events. Simula-

tions with cloud-resolving models show this as well, for instance by DERBYSHIRE et al. (2004); CHABOUREAU et al. (2004); WU et al. (2009); BÖING et al. (2012). Interestingly, parameters traditionally used for forecasting thunderstorms show different results for the role of mid-level humidity: The K Index (GEORGE, 1961), Jefferson index (JEFFERSON, 1966) and Swiss index (HUNTRIESER et al., 1997) predict a higher probability of thunderstorms with increasing mid-level humidity, whereas the Bradbury index (BRADBURY, 1977), the KO index (ANDERSSON et al., 1989) and the Potential Instability Index (VAN DELDEN, 2001) predict the opposite.

In addition to relative humidity, the vertical temperature gradient above the boundary layer may also be important. HOUSTON and NIYOGI (2007) found that steep lapse rates in the layer above the level of free convection favors the development of deep convective clouds. Furthermore, low-level wind shear may be of importance, as it helps to create organized regions of upward vertical motion in the boundary layer in the form of horizontal convective rolls.

Of all traditional forecast indices for non-severe thunderstorms, only the Swiss index (HUNTRIESER et al., 1997) incorporates wind shear and predicts an increasing likelihood of storms as it increases.

WECKWERTH et al. (1996) discussed the importance of the resulting thermodynamic variability in the boundary layer to convective initiation while BURTON et al. (2013) emphasized the importance of a realistic representation of boundary-layer and land-surface schemes for the simulation of deep convective clouds. They found a reduction of the amount of static energy available for convection if the moisture in the boundary layer is too well mixed. Energy is available for convection if a combination of boundary-layer and surface schemes allows a ‘reservoir’ of moisture to develop, assuming there is a trigger mechanism (BURTON et al., 2013).

In this study, we explore the relation between these and other parameters and the occurrence of electrified convection and seek to clarify the roles of wind shear, lapse rates, mid-level humidity, CAPE and CIN on the probability of thunderstorms.

We are the first to account for thunderstorm favorable environments in ERA-Interim reanalysis data without specifying the severity level of these storms as we are interested predominantly in thunderstorm initiation, but we also want to account for environments that are favorable for sustaining existing thunderstorms.

The investigation will help to create a basis for assessing the effects of climate change on the frequency of thunderstorms.

We start out with a description of methods and data in Section 2. In Section 3, we present the results, which we discuss in Section 4. In Section 5, we provide a summary and the conclusions.

2 Data and methods

To explore the relation between atmospheric parameters and the occurrence of convective storms, we use an ob-

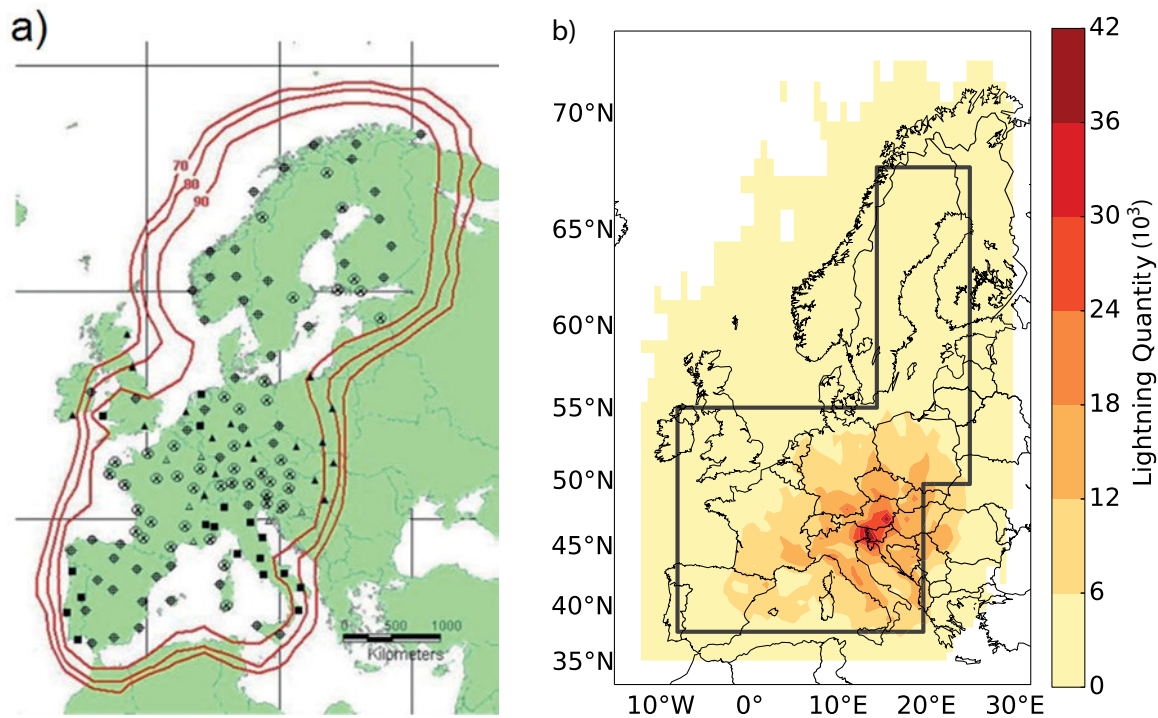


Figure 1: a) Ground Flash Detection Efficiency (in %) for the EUCLID network (August 2009) from DIENDORFER et al. (2010). The black symbols denote different sensor types. b) Number of lightning flashes during the period 2008 to 2013. The black polygon indicates the analysis domain situated within the EUCLID network coverage.

servational data set of lightning and a reanalysis dataset. Lightning serves as an indicator for the occurrence of deep, moist convection in our study. We are aware that a minority of deep-convective storms do not produce lightning (e.g., ZIPSER, 1994). This study is based on six years of data (1st January 2008 to 31 December 2013), which we will describe below.

2.1 Data

We assessed the occurrence of deep, moist convection using cloud-to-ground lightning detections by the European Cooperation of Lightning Detection (EUCLID), which is a cooperation between 23 European countries that provide lightning measurements from its national networks. DIENDORFER et al. (2010) and SCHULZ et al. (2014) provide a summary describing the network and its performance. EUCLID lightning data have been used in many scientific studies on lightning climatology (e.g., FEUDALE et al., 2013; POELMAN, 2014) and detection network comparisons (e.g., POHJOLA and MÄKELÄ, 2013).

Figure 1a shows the Flash Detection Efficiency estimation for the EUCLID network as of August 2009 from DIENDORFER et al. (2010), which is higher than 90 % in all of the participating countries. DIENDORFER et al. (2010) found that the median location accuracy is better than 500 m throughout Europe (not shown) and emphasized that the performance of the EUCLID network has steadily improved since its introduction.

We used hourly EUCLID data provided on a grid with a spacing of 0.25 ° latitude and longitude. Given that this is much larger than the location accuracy of the lightning network, the gridding should have a negligible effect on the results of this study.

Figure 1b depicts the distribution of the lightning data across Europe. The black polygon indicates the region of high lightning network coverage that was selected for the study.

Atmospheric data were obtained from the ERA-Interim global atmospheric reanalysis, produced at the European Centre for Medium-Range Weather Forecasts (ECMWF) (DEE et al., 2011). ERA-Interim is a state-of-the-art reanalysis dataset representing the atmosphere every six hours, available on a 0.75 ° × 0.75 ° horizontal grid, which yields 1138 grid points within the study area of Figure 1b. Over the entire 6 year period, 9 977 984 data points result in total. ERA-Interim has 60 vertical levels, however we used data interpolated to 28 pressure levels between 1000 hPa and 70 hPa, spaced 25 to 50 hPa apart.

2.2 Methods

To associate the lightning data with the reanalysis data, they were rescaled to the same spatial resolution (0.75 °), which meant that the lightning count was accumulated over 9 EUCLID grid-boxes. A lightning case is defined as the occurrence of two lightning strikes within two hours after the respective reanalysis time, i.e. within any

of the periods 00–02 UTC, 06–08 UTC, 12–14 UTC, 18–20 UTC. These two hour periods were chosen to be after the respective analysis times rather than centered around it (e.g., 23–01 UTC, etc.) so that the reanalysis data would represent the pre-convective rather than the post-convective environment. The time period of two hours was chosen based on a typical low- to mid-tropospheric wind speed in Central Europe of 10–15 m s⁻¹, which yields 2 hours as a typical timescale for a thunderstorm to leave the respective grid box.

Several parameters related to instability, moisture and bulk wind shear were computed from ERA-Interim for which temperature, humidity and wind data from the 28 available pressure levels were interpolated to 1 hPa vertical resolution. The computation of instability parameters depends on the virtual temperature profiles of adiabatically rising air parcels (BJERKNES, 1938), which were calculated with a numeric integration step of 1 hPa. The rising parcel source is 50 hPa above the local topography, which is typically within the planetary boundary layer. More details on the computation method are given by PISTOTNIK et al. (2016), who applied the same set of convection parameters to an evaluation of decadal climate hindcasts against ERA-Interim reanalyses. In the remainder of the article, we will discuss the parameters listed in Table 1.

3 Results

3.1 Distribution of CAPE and CIN

To start, we investigate the distribution of CAPE in our area of study, which can be expressed as a theoretical maximum updraft velocity w_{\max} (TRAPP et al., 2009; BROOKS, 2013). We find that nonzero CAPE is the exception rather than the rule: of all 9 977 984 data points no fewer than 6 901 513 (69.2 %) have CAPE = 0 J kg⁻¹. The distribution of the number of cases as a function of CAPE values shows a strong decrease (Figure 2a) for increasing CAPE values, indicating that high CAPE values are very rare. For instance, only in 0.087 % (8 557) of all cases does CAPE exceed a sizable value of 1800 J kg⁻¹. Lightning is a somewhat rare occurrence as well, as it was only observed in 1.8 % of all cases (182 536). The distribution of CAPE for all lightning cases is shown in Figure 2b.

In 18.7 % of all lightning cases (34 224) CAPE was 0 J kg⁻¹. Nevertheless, the fact that some CAPE is typically present when thunderstorms develop is shown by a local maximum at $w_{\max} = 15$ m s⁻¹ which corresponds to CAPE = 115 J kg⁻¹. The joint distribution of CAPE and CIN (excluding cases without CAPE; Figure 3a) shows that the atmosphere is usually in a state of both low CAPE and low absolute values of CIN. Both high CAPE and high absolute values of CIN are rare, and their combination is even rarer. For lightning cases (Figure 3b), the maximum of occurrences shifts towards higher CAPE and higher absolute values of CIN. A lo-

Table 1: Parameters computed from ERA-Interim reanalysis data.

| Parameter | Unit | Description |
|-------------------|----------------------|--|
| CAPE, | J kg ⁻¹ , | The Convective Available Potential Energy “is proportional to the kinetic energy that a parcel can gain from its environment as a result of the contribution of buoyancy to the vertical acceleration” (MARKOWSKI and RICHARDSON, 2011). |
| w_{\max} | (m s ⁻¹) | Theoretical parcel updraft speed, $w_{\max} = \sqrt{2 \cdot \text{CAPE}}$ (EMANUEL, 1994) sometimes called the <i>thermodynamic speed limit</i> (MARKOWSKI and RICHARDSON, 2011). |
| CIN, | J kg ⁻¹ , | Convective Inhibition. CIN has a negative value as it “is equal to the work that must be done against the stratification to lift a parcel of air to its level of free convection where the parcel becomes warmer than the environmental temperature” (MARKOWSKI and RICHARDSON, 2011). |
| w_{init} | (m s ⁻¹) | Theoretical speed to overcome CIN, $w_{\text{init}} = \sqrt{2 \cdot (-\text{CIN})}$. |
| LI _{min} | °C | Generalized Lifted Index calculated as the negative temperature excess at the level of maximum parcel buoyancy, not necessarily at 500 hPa in contrast to the classical Lifted Index defined by GALWAY (1956). |
| DLSmax | m s ⁻¹ | Magnitude of wind difference (i.e. bulk shear) between the wind interpolated to model surface height and 6 kilometers above the surface, or between the surface and that layer below 6 kilometers that yielded the highest wind difference. |
| MLSmax | m s ⁻¹ | As for DLSmax, but for 3 kilometer. |
| LLSmax | m s ⁻¹ | As for DLSmax, but for 1 kilometer. |
| rh850-500 | % | Average pressure-weighted relative humidity in the layer between 850 hPa and 500 hPa. |

cal maximum is located in the bin at 12–16 m s⁻¹ w_{\max} (or 72 to 128 J kg⁻¹ CAPE) and 4–8 m s⁻¹ w_{init} (or –8 to –32 J kg⁻¹ CIN).

3.2 Relation between lightning and instability

We consider the frequency of lightning f_L , which is defined as the fraction of lightning cases to all cases, as a function of CAPE (Figure 4a). As we may expect, f_L increases with increasing CAPE, however only up to ≈ 800 J kg⁻¹. Between 800 J kg⁻¹ and 2800 J kg⁻¹ f_L is approximately constant at ≈ 0.2 . Apparently, although higher CAPE supports stronger updraft speeds, the probability of convective initiation is not affected. That said, above CAPE = 2800 J kg⁻¹ ($w_{\max} \approx 75$ m s⁻¹) f_L increases further, but there is a high uncertainty, shown by the large 95 % confidence intervals.

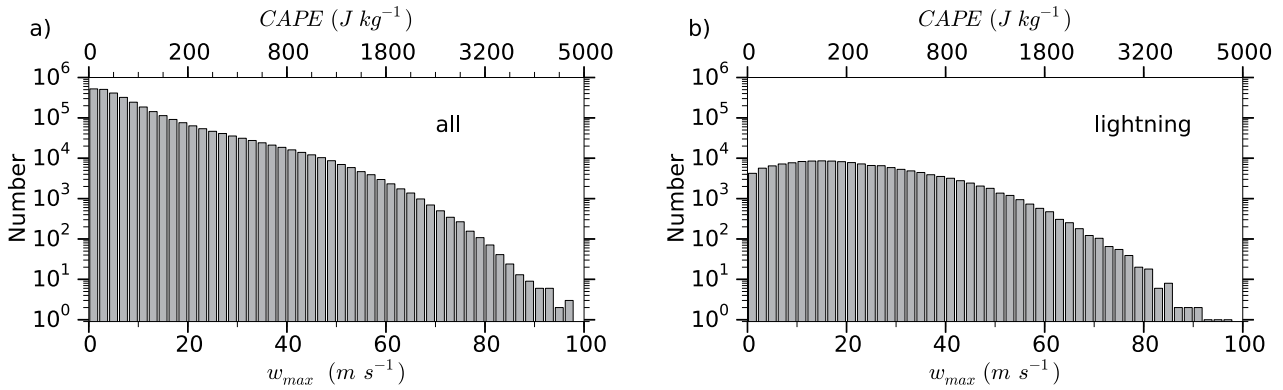


Figure 2: Distribution of CAPE for (a) all cases and (b) all lightning cases. Values of CAPE=0 J kg⁻¹ are removed. Note that the intervals used for the upper axes are different from the linear lower axes as the CAPE values represent the values of w_{max} calculated from CAPE = $w_{max}^2/2$.

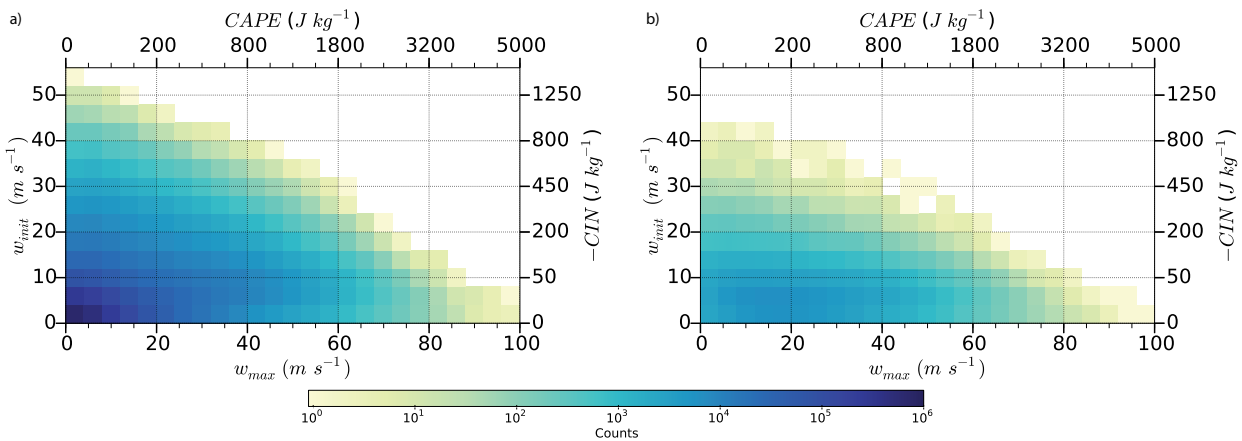


Figure 3: Joint distribution of w_{max} and w_{init} with corresponding CAPE and CIN for (a) all cases and (b) all lightning cases are illustrated. Again, only values of CAPE > 0 J kg⁻¹ are taken into account. Note that the intervals used for the upper and right axes are different from the linear lower and left axes as the CAPE and -CIN values represent the values for CAPE = $w_{max}^2/2$ and -CIN = $w_{init}^2/2$.

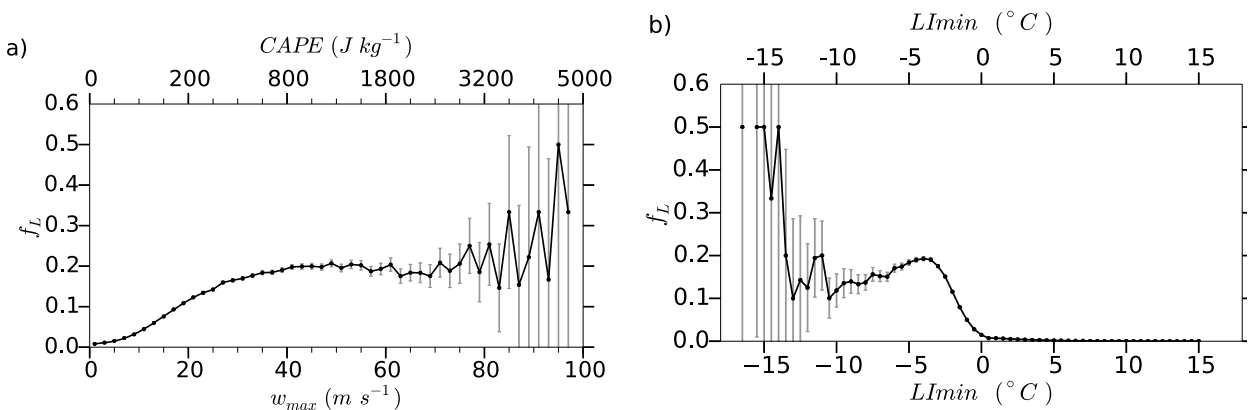


Figure 4: Relative frequency of lightning for (a) CAPE and (b) LI_{min} . The gray bars denote a 95 % confidence interval. Note that the intervals used for the upper axes in a) are different from the linear lower axes as the CAPE values represent the values for w_{max} calculated from CAPE = $w_{max}^2/2$.

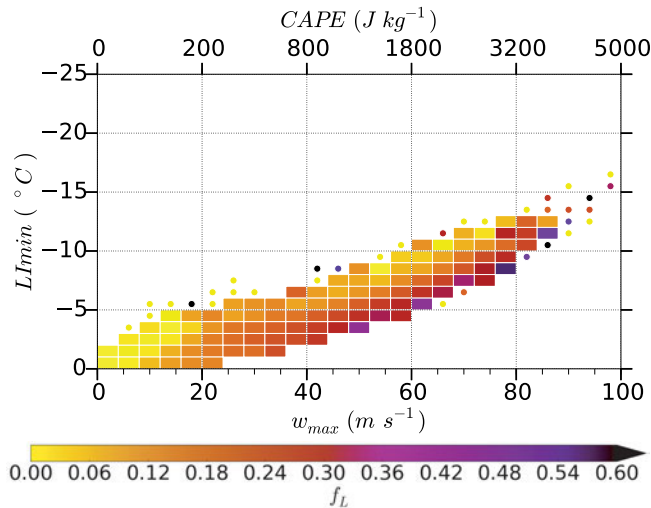


Figure 5: Relative frequency of lightning for the combination of CAPE and LI_{\min} . All bins containing less than 10 cases in total are depicted as dots. Note that the intervals used for the upper axes in a) are different from the linear lower axes as the CAPE values represent the values for w_{\max} calculated from $CAPE = w_{\max}^2/2$.

A similar analysis of f_L for the instability parameter LI_{\min} (see Figure 4b), initially shows an increase as LI_{\min} drops below 0°C , i.e. instability increases. The probability of lightning then reaches a local maximum with $f_L = 0.19$ at $LI_{\min} = -4.5^\circ\text{C}$. Interestingly, further increasing instability results not in an increase, but rather a decrease of f_L to around 0.12 at -11°C . For the lowest values for which some data was available, below -12°C , f_L again increases, but the large confidence intervals render this signal statistically insignificant.

The distribution of CAPE and LI_{\min} (Figure 5) comes in an elongated shape, since the two instability parameters are highly correlated. The joint analysis of these two parameters gives insight into the vertical distribution of parcel buoyancy. If, for a given value of CAPE, LI_{\min} is relatively low (i.e. very negative), the positive area that represents CAPE in a thermodynamic diagram is relatively short and bulky. If LI_{\min} is not so low (i.e. less negative) for the same given CAPE, the CAPE area is long and thin. Figure 5 shows that for any given value of CAPE, the highest probabilities of lightning are found for a less negative LI_{\min} , i.e. a long and thin CAPE area.

3.3 Relation between lightning and CIN

As might be expected, CIN close to zero and adequate CAPE are the most supportive for the development of deep convection and lightning (Figure 6). Lightning is most frequent for $CIN > -50\text{ J kg}^{-1}$ and $CAPE > 400\text{ J kg}^{-1}$, where f_L generally exceeds 0.2, with highest grid box values around 0.35. With low CAPE (below 400 J kg^{-1}), the highest frequency of lightning occurs for moderate CIN values (around -50 J kg^{-1}) rather than for CIN close to zero. This might be explained by the variability of CAPE on scales smaller than a grid cell of the ERA-Interim reanalysis model. There might

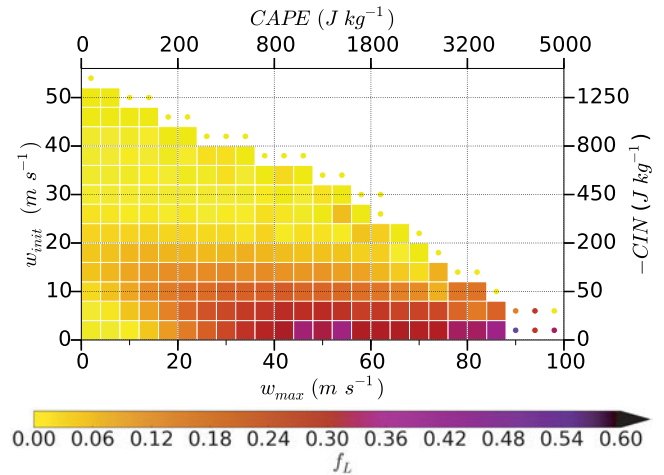


Figure 6: Relative frequency of lightning for the combination of CAPE and CIN. All bins containing less than 10 cases in total are depicted as dots. Note that the intervals used for the upper and right axes are different from the linear lower and left axes as the CAPE and $-CIN$ values represent the values for $CAPE = w_{\max}^2/2$ and $-CIN = w_{\text{init}}^2/2$.

be higher values of CAPE within a gridbox that cannot be resolved on a grid with a horizontal spacing of $0.75^\circ \times 0.75^\circ$. With moderate CIN, CAPE may build up at locations within the grid cell. When CIN is close to zero, however, convection will consume any CAPE early, thereby preventing sufficient CAPE to develop to sustain updrafts intense enough to support charge separation and lightning.

3.4 Relation between lightning and mid-level humidity

We find a strong relation between relative humidity in the low- to mid-troposphere and lightning occurrence. For high CAPE ($> 800\text{ J kg}^{-1}$) and high relative humidity (80%) between 850 and 500 hPa, the frequency of lightning increases to over 0.45 (Figure 7a).

Given adequate CAPE ($> 400\text{ J kg}^{-1}$), lightning occurrence strongly depends on the relative humidity in addition to CIN. Figure 7b, which only displays cases where $CAPE > 400\text{ J kg}^{-1}$, shows that a high lightning probability f_L occurs only for a combination of both low absolute values of CIN and high values of $rh_{850-500}$. In other words, low absolute CIN values are not a sufficient condition for storm occurrence. High relative humidity must be in place as well. In fact, it appears that the inhibiting effect of CIN is compensated by high relative humidity. Even though Figure 6 shows that the probability of lightning decreases to below 0.20 when CIN exceeds -50 J kg^{-1} , the subset of such cases with $CIN < -50\text{ J kg}^{-1}$ that also have $rh_{850-500} > 80\%$, are still associated with a high f_L , between 0.30 and 0.60 (Figure 7b).

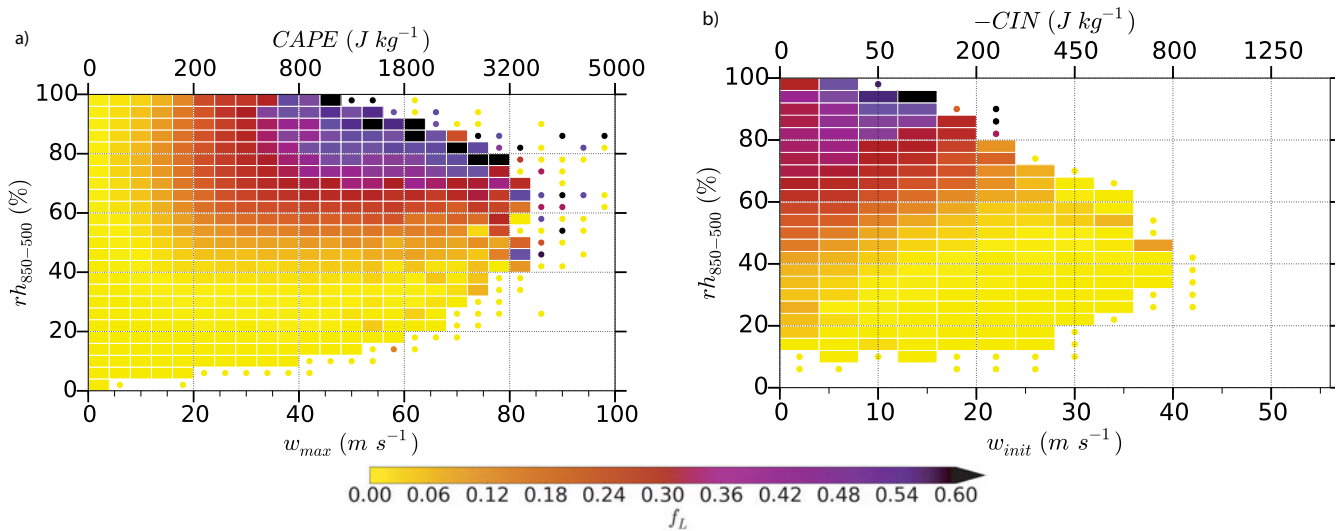


Figure 7: Relative frequency of lightning for (a) CAPE and the average relative humidity between 850 and 500 hPa ($rh_{850-500}$) and (b) $-CIN$ and $rh_{850-500}$ provided that $CAPE > 400 J kg^{-1}$. All bins containing fewer than 10 cases in total are depicted as dots. Note that the intervals used for the upper axes are different from the linear lower axes as the CAPE and $-CIN$ values represent the values calculated from $CAPE = w_{max}^2/2$ and $-CIN = w_{init}^2/2$.

3.5 Relation between lightning and lapse rate

The frequency of lightning depends on the lapse rate in the 850 to 500 hPa layer ($LR_{850-500}$), in that a maximum occurs at $6.5 K km^{-1}$ for a given CAPE value (Figure 8). For smaller lapse rates, the probability of storms is lower. This may be caused by the difficulty for convective clouds to maintain sufficient positive buoyancy as they mix with environmental air, as was demonstrated by [HOUSTON and NIYOGI \(2007\)](#). The decreasing probability for increasing lapse rates above the maximum is more puzzling at first sight as rising parcels can be expected to easily maintain high thermal buoyancy. However, there is a correlation between lapse rates and relative humidity, implying that environments with high lapse rates are deprived of sufficient moisture, so that water droplets in rising air parcels quickly evaporate and reduce the buoyancy. In addition, environments with strong lapse rates tend to have high absolute values of CIN.

3.6 Relation between lightning and vertical wind shear

Vertical wind shear influences lightning frequency. Figure 9a shows that, besides an increase of f_L with increasing CAPE for values up to $800 J kg^{-1}$, a bimodal dependence on DLS_{max} exists. Lightning tends to be relatively uncommon when DLS_{max} is moderate, i.e. within the area indicated by the black curve, and more common for both lower and higher values.

The bimodal dependence of f_L on shear can be explained by a combination of two effects. First, in very weak shear, towering cumulus clouds are not tilted and the likelihood of them developing into thunderstorms can be expected to be higher than in stronger shear. Second, strong deep-layer shear usually occurs in the vicinity of fronts and jets, since it is tied to the associated

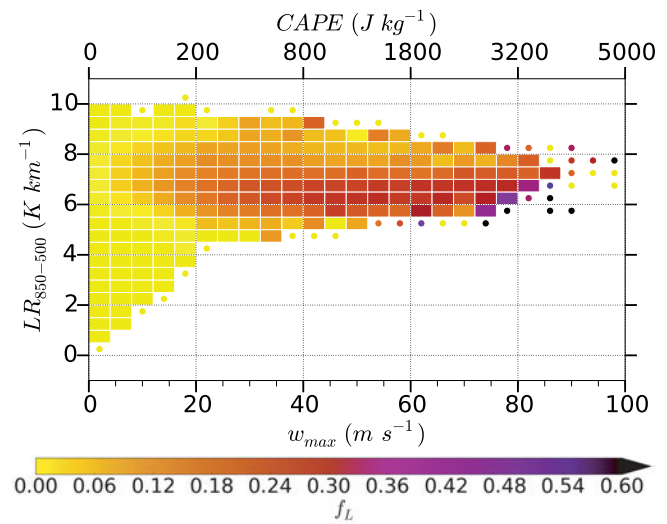


Figure 8: Relative frequency of lightning as a function of CAPE and lapse rate in the 850 to 500 hPa layer. All bins containing fewer than 10 cases in total are depicted as dots. Note that the intervals used for the upper axes are different from the linear lower axes as the CAPE values represent the values calculated from $CAPE = w_{max}^2/2$.

strong thermal gradient by virtue of the thermal wind balance. There, organized areas of upward vertical motion occur that help initiate and sustain well-organized convection, such as squall lines and supercells. Once such systems have formed, the strong shear also contributes to their maintenance. For intermediate values of DLS_{max} , the shear is detrimental to the initiation of isolated storms, but frontal systems are still too far away to create sufficient lift for initiation.

The dependence of f_L on MLS_{max} (Figure 9b) is similar to that of DLS_{max} . However, the bimodal signal of f_L for low and high values of MLS_{max} is not as pronounced

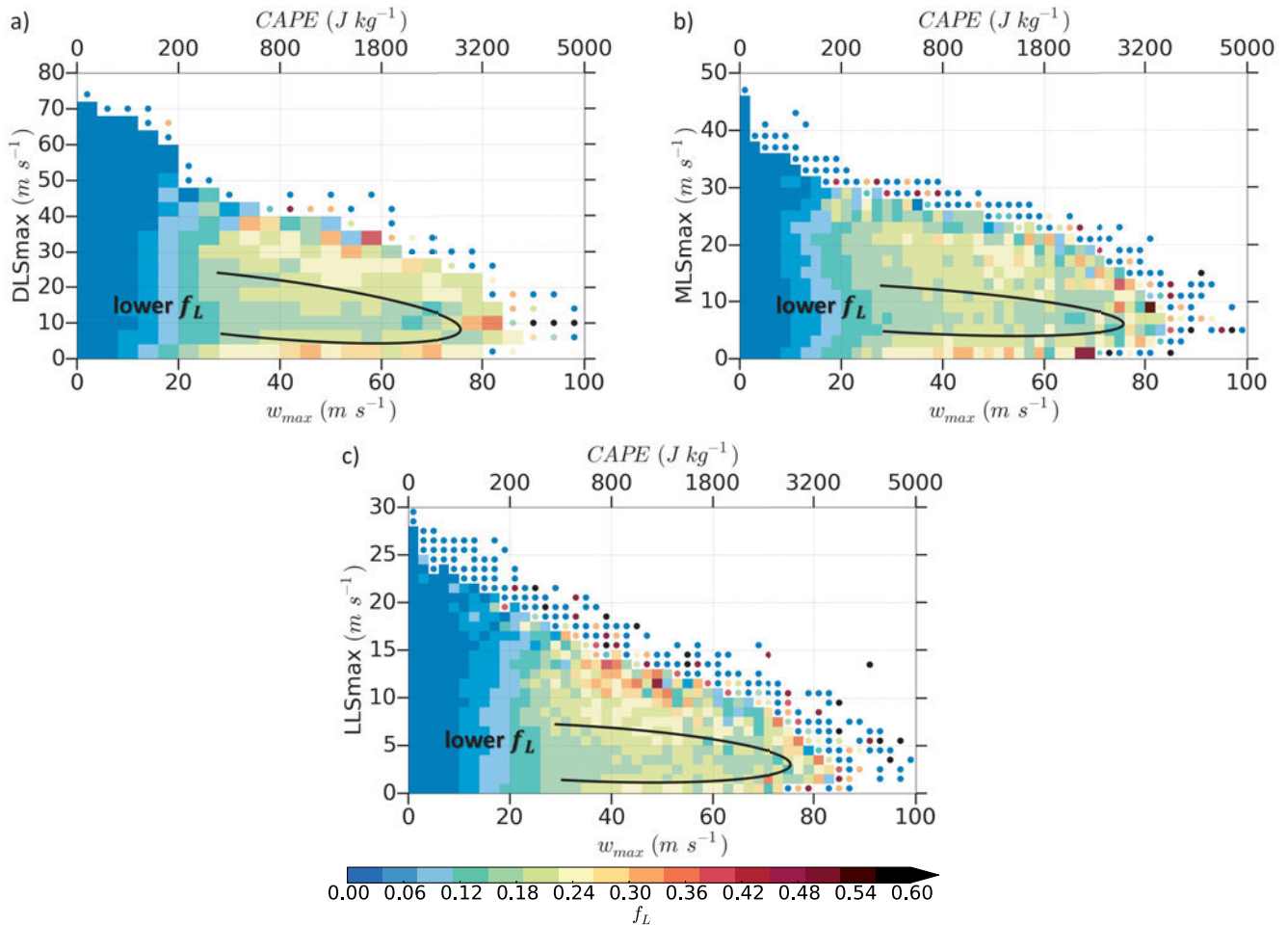


Figure 9: Relative frequency of lightning for CAPE (a) and maximum bulk shear between 0 km and 6 km (DLS_{max}), (b) maximum bulk shear between 0 km and 3 km (MLS_{max}) and (c) maximum bulk shear between 0 km and 1 km (LLS_{max}). The areas bounded by black contours separate regions of higher and lower f_L and are discussed in the text. The relative frequency of lightning is displayed as dots in those bins, where less than 10 cases occurred in the period 2008–2013. Note that the intervals used for the upper axes are different from the linear lower axes as the CAPE values represent the values calculated from $CAPE = w_{max}^2/2$.

as for DLS_{max} . In addition, the bimodal dependence of f_L on LLS_{max} is even less visible (Figure 9c). Higher f_L are found for values of $LLS_{max} \approx 10\text{--}16 \text{ m s}^{-1}$.

4 Discussion

4.1 Limitations

The present study is limited in a number of ways. First, we have not considered the effects of the type of land surface or the orography. Second, the resolution of the reanalysis data set may not be sufficient to resolve the immediate environment of thunderstorms; i.e. considerable variability may be present on scales smaller than the grid spacing. Third, although reanalyses are designed to represent the state of the atmosphere as consistently as possible with the available observations, they will deviate from the real atmosphere. Fourth, the area of this study was limited to central Europe, so that we cannot be certain that the findings of this study are valid in other regions. That said, we have limited the study to parameters that influence convective storms directly in

a physical way, which lends some confidence that the relationships will hold in other locations as well. We have not studied parameters that may influence storm development indirectly, such as the time of day, time of year, latitude or longitude. Last, because EUCLID detects little intracloud lightning, our study was limited to thunderstorms that produce at least two cloud-to-ground lightning strikes. This means that the small fraction of storms that produces only intracloud lightning was neglected. We have explored the sensitivity of the results to variations of the criterion for a lightning case, by varying the required number of lightning detections from 1 to 10. The absolute number of lightning cases decreases when this number is increased, but the relations between predictors and the frequency remain qualitatively similar. This also suggests that the slightly varying detection efficiency across the study area did not significantly influence the results.

4.2 Instability

The dependence of the frequency of lightning on CAPE shows that the vast majority of thunderstorms occur with

at least some instability. However, some storms occurred even with 0 J kg^{-1} CAPE or positive LI_{min} . This result may be explained by errors in the ERA-Interim reanalysis or the 0.75° grid spacing being insufficient to resolve local areas of instability.

A somewhat surprising result is that the relative frequency of lightning only increases until at a particular level of instability, regardless of whether it is expressed as CAPE or as a Lifted Index. In the latter case it even decreases after reaching a maximum at -4.5°C . [HAKLANDER and VAN DELDEN \(2003\)](#) did not find such a saturation for a study using proximity soundings in the Netherlands, probably because their data set did not include Lifted Index values below -5°C . The fact that such a maximum or saturation point is reached suggests that, in very unstable situations, other inhibiting effects become more likely. For example, the layer of air with near-adiabatic lapse rates that is required for such extreme instability, often creates both a capping inversion and constitutes a layer of dry air, which both inhibit thunderstorms. To test this hypothesis, we have computed the fraction of cases with $\text{CIN} > -300 \text{ J kg}^{-1}$ and $\text{RH} > 60\%$, i.e. the region that according to [Figure 7b](#) is favorable for convective initiation. For all moderately unstable cases with LI_{min} between -2°C and -5°C , this fraction is 0.53. For very unstable cases, with $\text{LI}_{\text{min}} < -5^\circ\text{C}$, this fraction is only 0.38, which proves that some factors that control initiation become less favorable for very unstable situations.

4.3 Wind shear

The bimodal dependence of lightning occurrence on wind shear has not been documented before. Very weak shear apparently helps rising buoyant plumes to develop into full-blown electrified storms. We suppose that shear affects the rate at which rising buoyant plumes mix with environmental air, a phenomenon that can be seen by the tearing of cumulus towers. Cumulus parameterizations schemes do not account for the effects of vertical wind shear as far as we are aware and might be improved by doing so.

4.4 Humidity and lapse rates

The suppressive effect of low relative humidity in the mid-troposphere on convective initiation is well-known in the tropical cyclone community. The presence of dry mid-tropospheric air from the Sahara is known to be detrimental to the genesis of tropical cyclones across the North Atlantic ([ZIPSER et al., 2009](#); [KOMAROMI, 2013](#)). We have now demonstrated that mid-latitude convection is also suppressed by a lack of moisture.

Scientists who study and develop cumulus parameterization schemes have long been aware of the inhibiting effect of dry air. For instance, [DERBYSHIRE et al. \(2004\)](#) write that ‘a dry mid-tropospheric profile (say 25% relative humidity) can suppress deep convection in favor of a shallow convection regime’. [WU et al. \(2009\)](#)

summarize several studies and conclude that the dry air is unfavorable for deep convection because its entrainment into cumulus clouds leads to strong evaporative cooling and negative buoyancy.

This finding is relevant for forecasters who look for layers of very high lapse rates in the mid-troposphere that in combination with high low-level humidity create high CAPE. Such layers are common, for instance, across the region often referred to as ‘Tornado alley’ in the central United States of America, or may be advected off the Spanish Plateau over western Europe where they are called a ‘Spanish Plume’ ([CARLSON and LUDLAM, 1968](#); [VAN DELDEN, 2001](#)). It is important to realize that the low mid-tropospheric humidity and the CIN that often accompanies these air-masses prevent convective initiation across a large area. From that perspective one can understand why convective initiation occurs first along the periphery of such air-masses, where the effects of low mid-tropospheric humidity and high absolute values of CIN are smaller, but CAPE is sufficient for the development of thunderstorms. Furthermore, many traditional predictors for thunderstorms do not take the effect of mid-level humidity into account, or worse, predict a higher probability of thunder with decreasing humidity in the mid-troposphere. This is the case for indices that represent potential instability in its definition as the vertical gradient of equivalent potential temperature (θ_e), such as the Bradbury index ([BRADBURY, 1977](#)), the KO-index ([ANDERSSON et al., 1989](#)) and the Potential Instability Index ([VAN DELDEN, 2001](#)) all of which showed poor to mediocre performance in studies comparing thunderstorm indices ([HAKLANDER and VAN DELDEN, 2003](#); [MANZATO, 2005](#); [KUNZ, 2007](#)).

5 Summary and conclusion

With this study we intended to learn how to detect favorable environments of thunderstorms in reanalysis datasets. We explored the relation between various parameters calculated from reanalysis data and observations of electrified convection over Europe. We were successful in identifying several factors that affect the likelihood of storms besides the mere presence of sufficient instability. These are the main conclusions:

1. An increase in instability is, above a certain threshold, not associated with an increasing likelihood of storms. CAPE of $200\text{--}400 \text{ J kg}^{-1}$ is sufficient to sustain electrified storms.
2. Low CIN and adequate CAPE are the most supportive for the development of thunderstorms and the probability for lightning is highest for $\text{CIN} > -50 \text{ J kg}^{-1}$ and $\text{CAPE} > 400 \text{ J kg}^{-1}$. Smaller values of CAPE (below 400 J kg^{-1}) show a higher frequency of lightning for moderate CIN values (around 50 J kg^{-1}) rather than for CIN close to zero.
3. Dry mid-level (850–500 hPa) air strongly suppresses convective storms. Even for low values of CIN and sufficient CAPE, the probability for storm initiation

is very low if the mid-troposphere is too dry (relative humidity below approximately 50 %).

4. Considering the lapse rates in the 850 hPa to 500 hPa layer, the highest probabilities for lightning were found for $LR_{850-500} \approx 6.5 \text{ K km}^{-1}$ in combination with CAPE values above 200–400 J kg⁻¹.
5. The ‘shape of the CAPE’, i.e. the shape of the positive area in a thermodynamic diagram affects the probability of lightning. For a given amount of CAPE, a ‘long and thin’ area is more favorable for lightning than a ‘short and fat’ area.
6. There are two different regimes of wind shear associated with a relatively high probability of electrified storms: one with very weak vertical wind shear, and one with high wind shear. With intermediate shear deep moist convection is somewhat less likely. This signal is found both for deep-layer and mid-level shear and less pronounced for low-level shear.

The results have relevance for forecasting in that the role of mid-level humidity and wind shear should be considered by forecasters in addition to a measure of buoyancy such as CAPE or the Lifted Index. We also identified a potential benefit for cumulus parameterizations to include the effects of wind shear, and provided a basis for further efforts to develop proxies for thunderstorms from climate models, reanalyses and numerical weather prediction models.

There are still a number of open questions that require further study. For instance, it is not given that the probabilities of lightning will be constant across the globe and this should be verified with datasets from other regions. It is also possible that further predictors, which we have not studied, contain information on the probability of lightning. Indeed, the work can be extended to include additional parameters.

Acknowledgments

We thank EUCLID for kindly providing the lightning data and ECMWF for the ERA-Interim reanalysis data. The authors would like to thank the reviewers for their detailed comments on the paper which helped to improve the work in many ways. Additionally, we would like to thank Prof. Dr. PETER HÖPPE who supported this study. The contributions of P. GROENEMEIJER and G. PISTOTNIK were funded by the German Bundesministerium für Bildung und Forschung (BMBF) through the research program “Mittelfristige Klimaprognosen” (MiKliP), grant FKZ: 01LP1117A.

References

- ALLEN, J.T., D.J. KAROLY, K.J. WALSH, 2014: Future Australian severe thunderstorm environments. Part I: A novel evaluation and climatology of convective parameters from two climate models for the late twentieth century. – *J. Climate* **27**, 3827–3847, DOI:10.1175/JCLI-D-13-00425.1.
- ANDERSSON, T., M. ANDERSSON, C. JACOBSSON, S. NILSSON, 1989: Thermodynamic indices for forecasting thunderstorms in southern Sweden. – *Meteor. Magazine* **118**, 141–146.
- BJERKNES, J., 1938: Saturated-adiabatic ascent of air through dry-adiabatically descending environment. – *Quart. J. Roy. Meteor. Soc.* **64**, 325–330, DOI:10.1002/qj.49706427509.
- BÖING, S.J., H.J. JONKER, A.P. SIEBESMA, W.W. GRABOWSKI, 2012: Influence of the subcloud layer on the development of a deep convective ensemble. – *J. Atmos. Sci.* **69**, 2682–2698, DOI:10.1175/JAS-D-11-0317.1.
- BRADBURY, T.A.M., 1977: The use of wet-bulb potential temperature charts. – *Meteor. Magazine* **106**, 233–251.
- BRIGHT, D.R., M.S. WANDISHIN, R.E. JEWELL, S.J. WEISS, 2005: A physically based parameter for lightning prediction and its calibration in ensemble forecasts. – In: Preprints, Conf. on Meteor. Appl. of Lightning Data. Citeseer.
- BROOKS, H., 2013: Severe thunderstorms and climate change. – 6th European Conference on Severe Storms 2011. Palma de Mallorca, Spain, *Atmos. Res.* **123**, 129–138, DOI:10.1016/j.atmosres.2012.04.002.
- BROOKS, H.E., J.W. LEEB, J.P. CRAVEN, 2003: The spatial distribution of severe thunderstorm and tornado environments from global reanalysis data. – *Atmos. Res.* **67–68**, 73–94, DOI:10.1016/S0169-8095(03)00045-0.
- BROWN, B.G., A.H. MURPHY, 1996: Verification of aircraft icing forecasts: The use of standard measures and meteorological covariates. – In: Preprints, 13th Conf. Probability and Statistics in the Atmospheric Sciences, San Francisco, California, USA, *Amer. Meteor. Soc.*, 251–252.
- BURTON, R.R., A. GADIAN, A. BLYTH, S. MOBBS, 2013: Modelling isolated deep convection: A case study from COPS. – *Meteorol. Z.* **22**, 433–443, DOI:10.1127/0941-2948/2013/0408.
- CARLSON, T.N., F.H. LUDLAM, 1968: Conditions for the occurrence of severe local storms. – *Tellus* **20**, 203–226, DOI:10.1111/j.2153-3490.1968.tb00364.x.
- CHABOUREAU, J.Y., F. GUICHARD, J.L. REDELSPERGER, J.À. LAFORE, 2004: The role of stability and moisture in the diurnal cycle of convection over land. – *Quart. J. Roy. Meteor. Soc.* **130**, 3105–3117, DOI:10.1256/qj.03.132.
- CRAVEN, J.P., H.E. BROOKS, 2004: Baseline Climatology of Sounding Derived Parameters Associated with Deep, Moist Convection. – *Nat. Wea. Dig.* **28**, 13–24.
- DEE, D., S. UPPALA, A. SIMMONS, P. BERRISFORD, P. POLI, S. KOBAYASHI, U. ANDRAE, M. BALMASEDA, G. BALSAMO, P. BAUER, OTHERS, 2011: The ERA-Interim reanalysis: Configuration and performance of the data assimilation system. – *Quart. J. Roy. Meteor. Soc.* **137**, 553–597, DOI:10.1002/qj.828.
- DEL GENIO, A.D., M.-S. YAO, J. JONAS, 2007: Will moist convection be stronger in a warmer climate?. – *Geophys. Res. Lett.* **34**, DOI:0.1029/2007GL030525.
- DERBYSHIRE, S.H., I. BEAU, P. BECHTOLD, J.Y. GRANDPEIX, J.M. PIRIOU, J.L. REDELSPERGER, P.M.M. SOARES, 2004: Sensitivity of moist convection to environmental humidity. – *Quart. J. Roy. Meteor. Soc.* **130**, 3055–3079, DOI:10.1256/qj.03.130.
- DIENDORFER, G., K.L. CUMMINS, W. SCHULZ, 2010: EUCLID – State of the Art Lightning Detection, 1–21.
- DIFFENBAUGH, N.S., M. SCHERER, R.J. TRAPP, 2013: Robust increases in severe thunderstorm environments in response to greenhouse forcing. – *Proceedings of the National Academy of Sciences* **110**, 16361–16366, DOI:10.1073/pnas.1307758110.
- DOSWELL III, C.A., 1987: The distinction between large-scale and mesoscale contribution to severe convection:

- A case study example. – *Wea. Forecast.* **2**, 3–16, DOI: [10.1175/1520-0434\(1987\)002<0003:TDBLSA>2.0.CO;2](https://doi.org/10.1175/1520-0434(1987)002<0003:TDBLSA>2.0.CO;2).
- DOSWELL III, C.A., H.E. BROOKS, R.A. MADDOX, 1996: Flash flood forecasting: An ingredients-based methodology. – *Wea. Forecast.* **11**, 560–581, DOI: [10.1175/1520-0434\(1996\)011<0560:FFFAIB>2.0.CO;2](https://doi.org/10.1175/1520-0434(1996)011<0560:FFFAIB>2.0.CO;2).
- EMANUEL, K.A., 1994: Atmospheric convection. – Oxford University Press on Demand.
- FEUDALE, L., A. MANZATO, S. MICHELETTI, 2013: A cloud-to-ground lightning climatology for north-eastern Italy. – *Advances in Science and Research* **10**, 77–84, DOI: [10.5194/asr-10-77-2013](https://doi.org/10.5194/asr-10-77-2013).
- GALWAY, J.G., 1956: The lifted index as a predictor of latent instability. – *Bull. Amer. Meteor. Soc.* **37**, 528–529.
- GENSINI, V.A., T.L. MOTE, 2014: Estimations of Hazardous Convective Weather in the United States Using Dynamical Downscaling. – *J. Climate* **27**, 6581–6589, DOI: [10.1175/JCLI-D-13-00777.1](https://doi.org/10.1175/JCLI-D-13-00777.1).
- GENSINI, V.A., T.L. MOTE, 2015: Downscaled estimates of late 21st century severe weather from CCSM3. – *Climatic Change* **129**, 307–321, DOI: [10.1007/s10584-014-1320-z](https://doi.org/10.1007/s10584-014-1320-z).
- GEORGE, J.J., 1961: Weather forecasting for aeronautics. – *Quart. J. Roy. Meteor. Soc.* **87**, 120–120, DOI: [10.1002/qj.49708737120](https://doi.org/10.1002/qj.49708737120).
- GROENEMEIJER, P., A. VAN DELDEN, 2007: Sounding-derived parameters associated with large hail and tornadoes in the Netherlands. – *Atmos. Res.* **83**, 473–487, DOI: [10.1016/j.atmosres.2005.08.006](https://doi.org/10.1016/j.atmosres.2005.08.006).
- HAKLANDER, A.J., A. VAN DELDEN, 2003: Thunderstorm predictors and their forecast skill for the Netherlands. – *Atmos. Res.* **67–68**, 273–299, DOI: [10.1016/S0169-8095\(03\)00056-5](https://doi.org/10.1016/S0169-8095(03)00056-5).
- HOUSTON, A.L., D. NIYOGI, 2007: The sensitivity of convective initiation to the lapse rate of the active cloud-bearing layer. – *Mon. Wea. Rev.* **135**, 3013–3032, DOI: [10.1175/MWR3449.1](https://doi.org/10.1175/MWR3449.1).
- HUNTRIESER, H., H. SCHIESSER, W. SCHMID, A. WALDVOGEL, 1997: Comparison of traditional and newly developed thunderstorm indices for Switzerland. – *Wea. Forecast.* **12**, 108–125, DOI: [10.1175/1520-0434\(1997\)012<0108:COTAND>2.0.CO;2](https://doi.org/10.1175/1520-0434(1997)012<0108:COTAND>2.0.CO;2).
- JEFFERSON, G., 1966: Letter to the editor. – *Meteor. Magazine* **95**, 381–382.
- JOHNS, R.H., C.A. DOSWELL III, 1992: Severe local storms forecasting. – *Wea. Forecast.* **7**, 588–612, DOI: [10.1175/1520-0434\(1992\)007<0588:SLSF>2.0.CO;2](https://doi.org/10.1175/1520-0434(1992)007<0588:SLSF>2.0.CO;2).
- KOMAROMI, W.A., 2013: An investigation of composite dropsonde profiles for developing and nondeveloping tropical waves during the 2010 PREDICT field campaign. – *J. Atmos. Sci.* **70**(2), 542–558, DOI: [10.1175/JAS-D-12-052.1](https://doi.org/10.1175/JAS-D-12-052.1).
- KUNZ, M., 2007: The skill of convective parameters and indices to predict isolated and severe thunderstorms. – *Natural Hazards Earth Sys. Sci.* **7**, 327–342.
- MANZATO, A., 2005: The Use of Sounding-Derived Indices for a Neural Network Short-Term Thunderstorm Forecast. – *Wea. Forecast.* **20**, 896–917, DOI: [10.1175/WAF898.1](https://doi.org/10.1175/WAF898.1).
- MARKOWSKI, P., Y. RICHARDSON, 2011: Mesoscale Meteorology in Midlatitudes, Volume 2. – John Wiley & Sons.
- McNULTY, R.P., 1978: On upper tropospheric kinematics and severe weather occurrence. – *Mon. Wea. Rev.* **106**, 662–672, DOI: [10.1175/1520-0493\(1978\)106<0662:OUTKAS>2.0.CO;2](https://doi.org/10.1175/1520-0493(1978)106<0662:OUTKAS>2.0.CO;2).
- NIALL, S., K. WALSH, 2005: The impact of climate change on hailstorms in southeastern Australia. – *Int. J. Climatol.* **25**, 1933–1952, DOI: [10.1002/joc.1233](https://doi.org/10.1002/joc.1233).
- PISTOTNIK, G., P. GROENEMEIJER, R. SAUSEN, 2016: Validation of Convective Parameters in MPI-ESM Decadal Hindcasts (1971–2012) against ERA-Interim Reanalyses. – *Meteorol. Z.* DOI: [10.1127/metz/2016/0649](https://doi.org/10.1127/metz/2016/0649).
- POELMAN, D.R., 2014: A 10-year study on the characteristics of thunderstorms in Belgium based on cloud-to-ground lightning data. – *Mon. Wea. Rev.* **142**, 4839–4849, DOI: [10.1175/MWR-D-14-00202.1](https://doi.org/10.1175/MWR-D-14-00202.1).
- POHJOLA, H., A. MÄKELÄ, 2013: The comparison of GLD360 and EUCLID lightning location systems in Europe. – *Atmos. Res.* **123**, 117–128, DOI: [10.1016/j.atmosres.2012.10.019](https://doi.org/10.1016/j.atmosres.2012.10.019).
- SANDER, J., 2011: Extremwetterereignisse im Klimawandel Bewertung der derzeitigen und zukünftigen Gefährdung. – Dissertation, LMU München.
- SANDER, J., J. EICHNER, E. FAUST, M. STEUER, 2013: Rising variability in thunderstorm-related US losses as a reflection of changes in large-scale thunderstorm forcing. – *Weather, Climate, and Society* (2013), DOI: [10.1175/WCAS-D-12-00023.1](https://doi.org/10.1175/WCAS-D-12-00023.1).
- SCHULTZ, D.M., J.V. CORTINAS JR, C.A. DOSWELL III, 2002: Comments on “An operational ingredients-based methodology for forecasting midlatitude winter season precipitation”. – *Wea. Forecast.* **17**, 160–167, DOI: [10.1175/1520-0434\(2002\)017<0160:COAOIB>2.0.CO;2](https://doi.org/10.1175/1520-0434(2002)017<0160:COAOIB>2.0.CO;2).
- SCHULZ, W., S. PEDEBOY, C. VERGEINER, E. DEFER, W. RISSON, 2014: Validation of the EUCLID LLS during HyMeX SOP1. – In: Proceedings, International Lightning Detection Conference ILDC.
- TAYLOR, K.E., R.J. STOUFFER, G.A. MEEHL, 2012: An overview of CMIP5 and the experiment design. – *Bull. Amer. Meteor. Soc.* **93**, 485–498, DOI: [10.1175/BAMS-D-11-00094.1](https://doi.org/10.1175/BAMS-D-11-00094.1).
- THOMPSON, R.L., R. EDWARDS, J.A. HART, K.L. ELMORE, P. MARKOWSKI, 2003: Close proximity soundings within supercell environments obtained from the Rapid Update Cycle. – *Wea. Forecast.* **18**, 1243–1261, DOI: [10.1175/1520-0434\(2003\)018<1243:CPSWSE>2.0.CO;2](https://doi.org/10.1175/1520-0434(2003)018<1243:CPSWSE>2.0.CO;2).
- TIPPETT, M.K., A.H. SOBEL, S.J. CAMARGO, 2012: Association of us tornado occurrence with monthly environmental parameters. – *Geophys. Res. Lett.* **39**, DOI: [10.1029/2011GL050368](https://doi.org/10.1029/2011GL050368).
- TIPPETT, M.K., J.T. ALLEN, V.A. GENSINI, H.E. BROOKS, 2015: Climate and Hazardous Convective Weather. – *Current Climate Change Reports* 60–73, DOI: [10.1007/s40641-015-0006-6](https://doi.org/10.1007/s40641-015-0006-6).
- TRAPP, R.J., N.S. DIFFENBAUGH, H.E. BROOKS, M.E. BALDWIN, E.D. ROBINSON, J.S. PAL, 2007a: Changes in severe thunderstorm environment frequency during the 21st century caused by anthropogenically enhanced global radiative forcing. – *Proceedings of the National Academy of Sciences* **104**, 19719–19723, DOI: [10.1073/pnas.0705494104](https://doi.org/10.1073/pnas.0705494104).
- TRAPP, R.J., B.A. HALVORSON, N.S. DIFFENBAUGH, 2007b: Tele-scoping, multimodel approaches to evaluate extreme convective weather under future climates. – *J. Geophys. Res. Atmos.* (1984–2012) **112**(D20), DOI: [10.1029/2006JD008345](https://doi.org/10.1029/2006JD008345).
- TRAPP, R.J., N.S. DIFFENBAUGH, A. GLUHOVSKY, 2009: Transient response of severe thunderstorm forcing to elevated greenhouse gas concentrations. – *Geophys. Res. Lett.* **36**, DOI: [10.1029/2008GL036203](https://doi.org/10.1029/2008GL036203).
- TRAPP, R.J., E.D. ROBINSON, M.E. BALDWIN, N.S. DIFFENBAUGH, B.R. SCHWEDLER, 2011: Regional climate of hazardous convective weather through high-resolution dynamical downscaling. – *Climate Dyn.* **37**, 677–688, DOI: [10.1007/s00382-010-0826-y](https://doi.org/10.1007/s00382-010-0826-y).
- VAN DELDEN, A., 2001: The synoptic setting of thunderstorms in western Europe. – *Atmos. Res.* **56**, 89–110, DOI: [10.1016/S0169-8095\(00\)00092-2](https://doi.org/10.1016/S0169-8095(00)00092-2).
- VAN DEN BROEKE, M.S., D.M. SCHULTZ, R.H. JOHNS, J.S. EVANS, J.E. HALES, 2005: Cloud-to-ground lightning production in strongly forced, low-instability convective lines associated with damaging wind. – *Wea. Forecast.* **20**, 517–530, DOI: [10.1175/WAF876.1](https://doi.org/10.1175/WAF876.1).

- VAN KLOOSTER, S.L., P.J. ROEBBER, 2009: Surface-based convective potential in the contiguous united states in a business-as-usual future climate. – *J. Climate* **22**, 3317–3330, DOI: [10.1175/2009JCLI2697.1](https://doi.org/10.1175/2009JCLI2697.1).
- WAPLER, K., F. HARNISCH, T. PARDOWITZ, F. SENF, 2015: Characterisation and predictability of a strong and a weak forcing severe convective event – a multi-data approach. – *Meteorol. Z.* **24**, 393–410, DOI: [10.1127/metz/2015/0625](https://doi.org/10.1127/metz/2015/0625).
- WECKWERTH, T.M., J.W. WILSON, R.M. WAKIMOTO, 1996: Thermodynamic variability within the convective boundary layer due to horizontal convective rolls. – *Mon. Wea. Rev.* **124**, 769–784, DOI: [10.1175/1520-0493\(1996\)124<0769:TVWTCB>2.0.CO;2](https://doi.org/10.1175/1520-0493(1996)124<0769:TVWTCB>2.0.CO;2).
- WEISMAN, M.L., J.B. KLEMP, 1984: The Structure and Classification of Numerically Simulated Convective Storms in Directionally Varying Wind Shears. – *Mon. Wea. Rev.* **112**, 2479–2498, DOI: [10.1175/1520-0493\(1984\)112<2479:TSACON>2.0.CO;2](https://doi.org/10.1175/1520-0493(1984)112<2479:TSACON>2.0.CO;2).
- WU, C.-M., B. STEVENS, A. ARAKAWA, 2009: What controls the transition from shallow to deep convection?. – *J. Atmos. Sci.* **66**, 1793–1806, DOI: [10.1175/2008JAS2945.1](https://doi.org/10.1175/2008JAS2945.1).
- ZHANG, Y., S.A. KLEIN, 2010: Mechanisms affecting the transition from shallow to deep convection over land: Inferences from observations of the diurnal cycle collected at the arm southern great plains site. – *J. Atmos. Sci.* **67**, 2943–2959, DOI: [10.1175/2010JAS3366.1](https://doi.org/10.1175/2010JAS3366.1).
- ZIPSER, E.J., 1994: Deep cumulonimbus cloud systems in the tropics with and without lightning. – *Mon. Wea. Rev.* **122**, 1837–1851, DOI: [10.1175/1520-0493\(1994\)122<1837:DCCSIT>2.0.CO;2](https://doi.org/10.1175/1520-0493(1994)122<1837:DCCSIT>2.0.CO;2).
- ZIPSER, E.J., C.H. TWOHY, S.C. TSAY, K.L. THORNHILL, S. TANELLI, R. ROSS, T.N. KRISHNAMURTI, Q. JI, G. JENKINS, S. ISMAIL, N.C. HSU, R. HOOD, G.M. HEYMSFIELD, A. HEYMSFIELD, J. HALVERSON, H.M. GOODMAN, R. FERRARE, J.P. DUNION, M. DOUGLAS, R. CIFELLI, G. CHEN, E.V. BROWELL, B. ANDERSON, 2009: The Saharan air layer and the fate of African easterly waves: NASA's AMMA field study of tropical cyclogenesis. – *Bull. Amer. Meteor. Soc.* **90**, 1137–1156, DOI: [10.1175/2009BAMS2728.1](https://doi.org/10.1175/2009BAMS2728.1).